Debonding Microprocess and interfacial strength in ZrC Nanoparticle-Filled AA1100 Alloy Matrix Composites using RVE approach

[1]B. Kotiveera Chari and A. Chennakesava Reddy[2]

[1]Professor, Department of Mechanical Engineering, NIT, Warangal, Andhra Pradesh, India
[2]Assistant Professor, Department of Mechanical Engineering, MJ College of Engineering and Technology, Hyderabad, India
dr_acreddy@yahoo.com

Abstract: *A hexagonal array unit cell/spherical ZrC nanoparticle RVE models were used to estimate micromechanical behavior and interfacial debonding in AA1100/ZrC composites. The AA1100/ZrC particulate metal matrix composites were fabricated at different volume fractions of ZrC. The heat treated specimens were tensile tested. The frqcture of ZrC nanoparticle was observed in all the composites.*

Keywords: AA1100*, zirconium carbide, spherical nanoparticle, RVE model, finite element analysis, particle fracture.*

1. INTRODUCTION

Representative volume element (RVE) approach is a novel method for simulating the behavior of composite materials by making use of the capabilities of a finite element software package. Particles reinforced metal matrix composites exhibits heterogeneity with regard to microstructure. This heterogeneity can be attributed to the presence of dispersed particulates in a matrix and the mechanical behavior of these composites largely depends on the size, shape and properties of these particulates. Conducting a large number of experiments in an effort to determine the macroscopic response of these materials, on a number of material samples, for various phase properties, volume fraction and loading conditions are difficult and expensive. The RVE is defined as the minimum volume of laboratory scale specimen such that the results obtained from this specimen can still be regarded as from a representative of the continuum. A variety of shapes such as spherical [1-3], ellipsoidal [4], hexagonal [5-8], rectangular [9-10] and rhombus [11-14] of the reinforced particles at different volume fractions were studied and the results from a unit cell with uniformly distributed particles were compared. Hill [15], Hashin [16] and AC Reddy [2, 4, 5, 9, 11, 12] played an important role in introducing and developing this approach that takes mechanical properties like elastic modulus, Poisson's ratio, mass density etc of the individual phases to predict the macroscopic properties of the heterogeneous material. A study was conducted on the silane interfacial effect on the fracture process of embedded single E-glass fiber [17]. The interfacial reinforcement reflects the progressed fracture rather than the instantaneous fracture.

Like most carbides of refractory metals, zirconium carbide is sub-stoichiometric, i.e., it contains carbon vacancies. At carbon contents higher than approximately ZrC0.98 the material contains free carbon. ZrC is stable for a carbon-to-metal ratio ranging from 0.65 to 0.98. ZrC seems suitable for use in re-entry vehicles, rocket/SCRAM jet engines or supersonic vehicles in which low densities and high temperatures load-bearing capabilities are crucial requirements. The purpose of this paper was to analyze debonding microprocess and interfacial interfacial strength of AA1100 alloy/zirconium carbide (ZrC) nanoparticle composites using RVE model through finite Element analysis. Shape of the reinforced particle considered in this work is a spherical. The periodic particle distribution was hexagonal array.

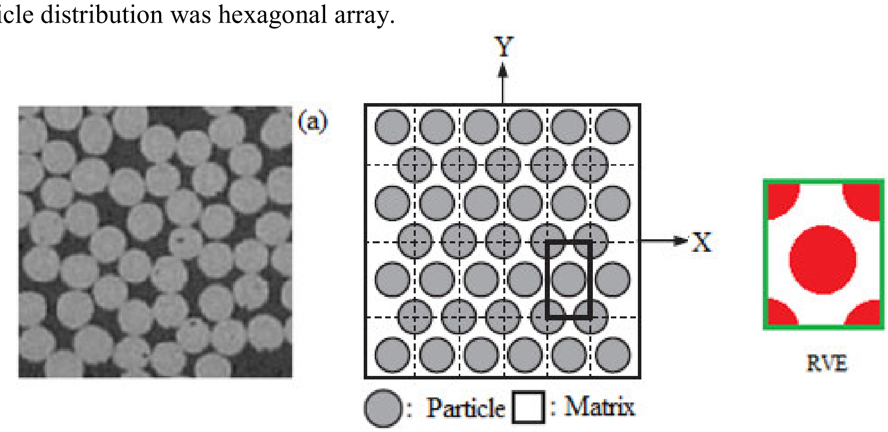

Figure 1: A hexagonal RVE containing a spherical nanoparticle.

2. THEORETICAL BACKGROUND

The strains along x- and y-directions can be determined as using the following equations:

$$\varepsilon_y = -\left(\frac{v_{xy}}{E_x} + \frac{1}{E_z}\right) P = \frac{\Delta y}{a} \tag{1}$$

$$\varepsilon_x = \left(\frac{1}{E_x} - \frac{1}{E_z}\right) P = \frac{\Delta x}{a} \tag{2}$$

The effective elastic moduli and Poisson's ratio in the transverse direction (xy-plane) as follows:

$$E_x = \frac{1}{\frac{\Delta x}{Pa}+\frac{1}{E_z}} \text{ and } E_y = \frac{1}{\frac{\Delta y}{Pa}+\frac{1}{E_z}} \tag{3}$$

$$v_{xy} = \left(\frac{\Delta y}{Pa} + \frac{1}{E_z}\right) / \left(\frac{\Delta x}{Pa} + \frac{1}{E_z}\right) \tag{4}$$

Once the change in lengths along x- and y- direction (Δx and Δy) are determined for the square RVE from the FEA, E_y and E_x and v_{xy} can be determined from Eqs. (3) and (4), correspondingly. Considering adhesion, formation of precipitates, particle size, agglomeration, voids/porosity, obstacles to the dislocation, and the interfacial reaction of the particle/matrix, the formula for the strength of composite is stated below:

$$\sigma_c = \left[\sigma_m \left\{\frac{1-(v_p+v_v)^{2/3}}{1-1.5(v_p+v_v)}\right\}\right] e^{m_p(v_p+v_v)} + k d_p^{-1/2} \tag{5}$$

$$k = E_m m_m / E_p m_p$$

where, v_v and v_p are the volume fractions of voids/porosity and nanoparticles in the composite respectively, m_p and m_m are the possion's ratios of the nanoparticles and matrix respectively, d_p is the mean nanoparticle size (diameter) and E_m and E_p is elastic moduli of the matrix and the particle respectively. Elastic modulus (Young's modulus) is a measure of the stiffness of a material and is a quantity used to characterize materials. Elastic modulus is the same in all orientations for isotropic materials. Anisotropy can be seen in many composites.

The upper-bound equation is given by

$$\frac{E_c}{E_m} = \left(\frac{1-{v_v}^{2/3}}{1-{v_v}^{2/3}+v_v}\right) + \frac{1+(\delta-1){v_p}^{2/3}}{1+(\delta-1)({v_p}^{2/3}-v_p)} \tag{6}$$

The lower-bound equation is given by

$$\frac{E_c}{E_m} = 1 + \frac{v_p - v_p}{\delta/(\delta-1)-(v_p+v_v)^{1/3}} \tag{7}$$

where, $\delta = E_p / E_m$.

The transverse modulus is given by

$$E_t = \frac{E_m E_p}{E_m + E_p(1-{v_p}^{2/3})/{v_p}^{2/3}} + E_m\left(1 - {v_p}^{2/3} - {v_v}^{2/3}\right) \tag{8}$$

3. MATERIALS METHODS

The matrix material was AA1100 aluminum alloy. The reinforcement material was ellipsoidal zirconium carbide (ZrC) nanoparticles of average size 100nm. The mechanical properties of materials used in the present work are given in table 1.

Table 1: Mechanical properties of AA1100 matrix and ZrC nanoparticles

Property	AA1100	ZrC
Density, g/cc	2.71	6.73
Elastic modulus, GPa	68.9	430
Ultimate tensile strength, MPa	110	874
Poisson's ratio	0.33	0.25

AA1100 alloy/ZRC composites were manufactured by the stir casting process and low pressure casting technique with argon gas at 3.0 bar. The composite samples were give solution treatment and cold rolled to the predefined size of tensile specimens. The heat-treated samples were machined to get flat-rectangular specimens (figure 2) for the tensile tests. The tensile specimens were placed in the grips of a Universal Test Machine (UTM) at a specified grip separation and pulled until failure. The test speed was 2 mm/min (as for ASTM D3039). A strain gauge was used to determine elongation.

In this research, a cubical representative volume element (RVE) was implemented to analyze the tensile behavior AA1100/ZrC nanoparticle composites at three (10%, 20% and 30%) volume fractions of ZrC. The large strain PLANE183 element was used in the matrix in all the models. In order to model the adhesion between the matrix and the particle, a CONTACT 172 element was used.

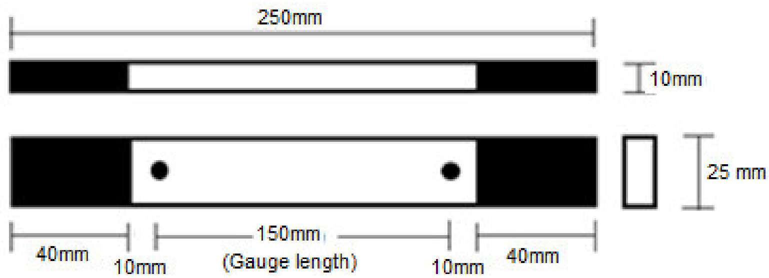

Figure 2: Shape and dimensions of tensile specimen

4. RESULTS AND DISCUSSION

The micromechanical behavior is discussed in terms of tensile elastic moduli, E_x, shear modulus, G_{xy} and major Poisson's ratio, v_{xy}. The fracture behavior is conversed in terms of interface debonding and particle fracture.

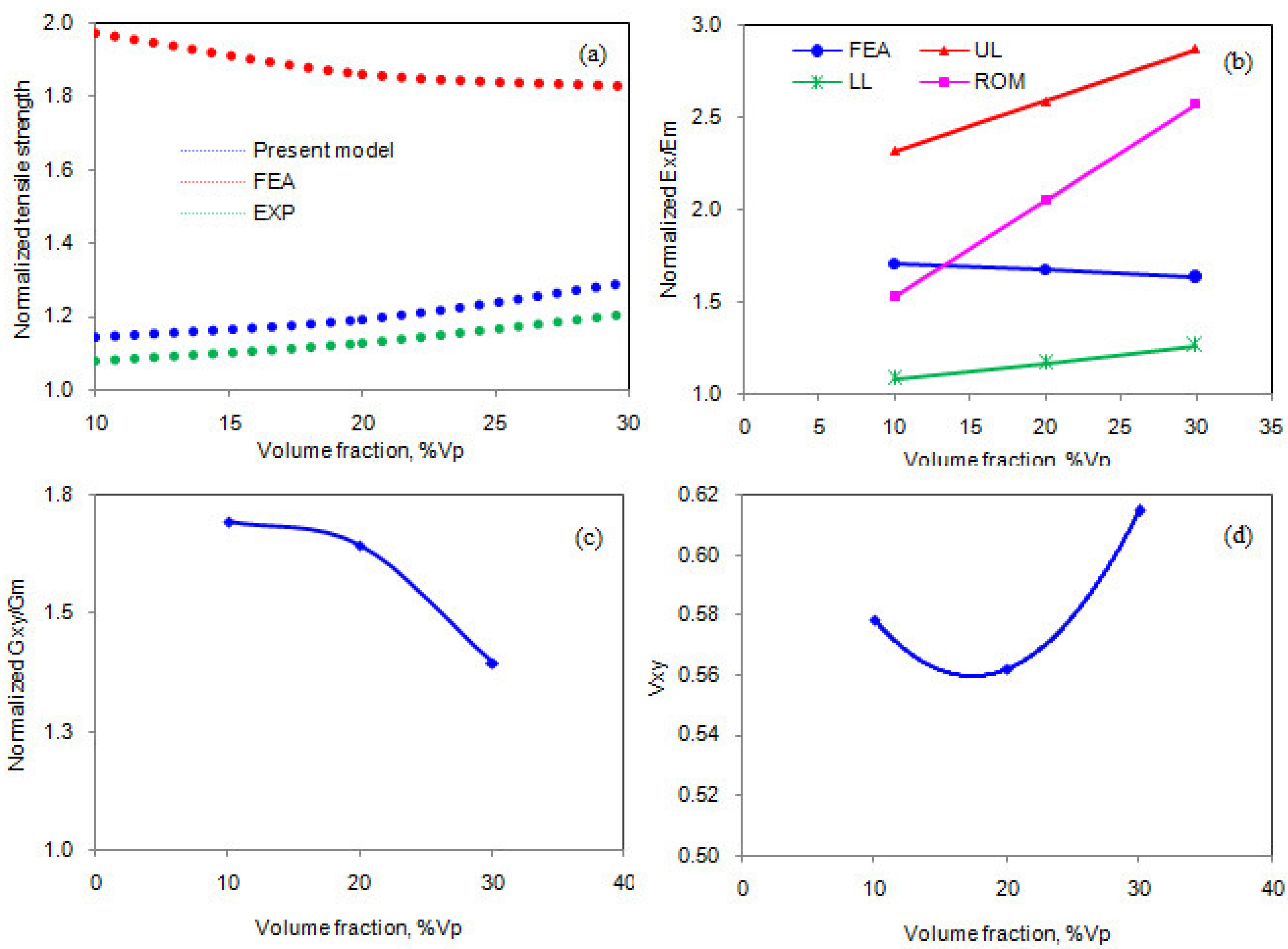

Figure 3: Effect of volume fraction on micromechanical behavior of AA1100/ZrC composites.

4.1 Micromechanical Behavior

Figure 3a depicts the normalized tensile strengths of the AA1100 alloy/ZrC composites obtained by FEA, present mathematical model, and experimental test. The tensile strength is normalized with ultimate tensile strength of AA1100 alloy matrix. The mathematical model includes the effect of voids present in the composite. The difference between the FEA results and the test results varies from 68 to 99 MPa. This difference can be attributed to the presence of voids in the composites and distribution of particles in the matrix. The distribution of ZrC nanoparticles was greatly affected by the density difference between the nanoparticles and the matrix. The difference between the results obtained from present mathematical model and the experimentation varies from 7 to10 MPa. The difference between the results obtained from present mathematical model and the FEA varies from 58 to 91 MPa. This is due to the ignorance of voids and agglomeration of ZrC nanoparticles in the (RVE models. The test and mathematical results of tensile strength increase with increase of volume fraction of ZrC in the composite; while the FEA results decrease with increase of volume fraction of ZrC.

The normalized elastic modulus is shown in figure 3b. The elastic modulus is normalized with the elastic modulus of AA1100 alloy matrix. From the results obtained from the mathematical computation and test procedure, the stiffness of the composites increases with increase of volume fraction of ZrC. The FEA results show decreasing trend of stiffness with increase in content of ZrC. The upper limit (UL) values computed by the present mathematical model are higher than those values obtained by the 'Role of Mixtures (ROM)'and FEA. This is because of consideration of voids in the present mathematical model. The shear strength of the composites decreases with increase in the volume fraction of ZrC (figure 3c). The major Poisson's ratio increases with increase of volume fraction of ZrC particles above 20% of ZrC (figure 3d).

4.2 Fracture Analysis

If the particle deforms in an elastic manner (according to Hooke's law) then,

$$\tau = \frac{n}{2}\sigma_p \quad (9)$$

where σ_p is the particle stress. If particle fracture occurs when the stress in the particle reaches its ultimate tensile strength, $\sigma_{p,uts}$, then setting the boundary condition at

$$\sigma_p = \sigma_{p,\,uts} \quad (10)$$

The relationship between the strength of the particle and the interfacial shear stress is such that if

$$\sigma_{P,uts} < \frac{2\tau}{n} \quad (11)$$

Then the particle will fracture. From the figure 4b, it is observed that the ZrC nanoparticle was fractured as the condition in Eq.(11) is satisfied. For the interfacial debonding/yielding to occur, the interfacial shear stress reaches its shear strength:

$$\tau = \tau_{max} \quad (12)$$

For particle/matrix interfacial fracture can occur if the following condition is satisfied:

$$\tau_{max} < \frac{n\sigma_p}{2} \quad (13)$$

It is observed from figure 4a that the interfacial debonding does not occur between ZrC nanoparticle and AA1100 alloy matrix as the condition in Eq.(13) is not satisfied.

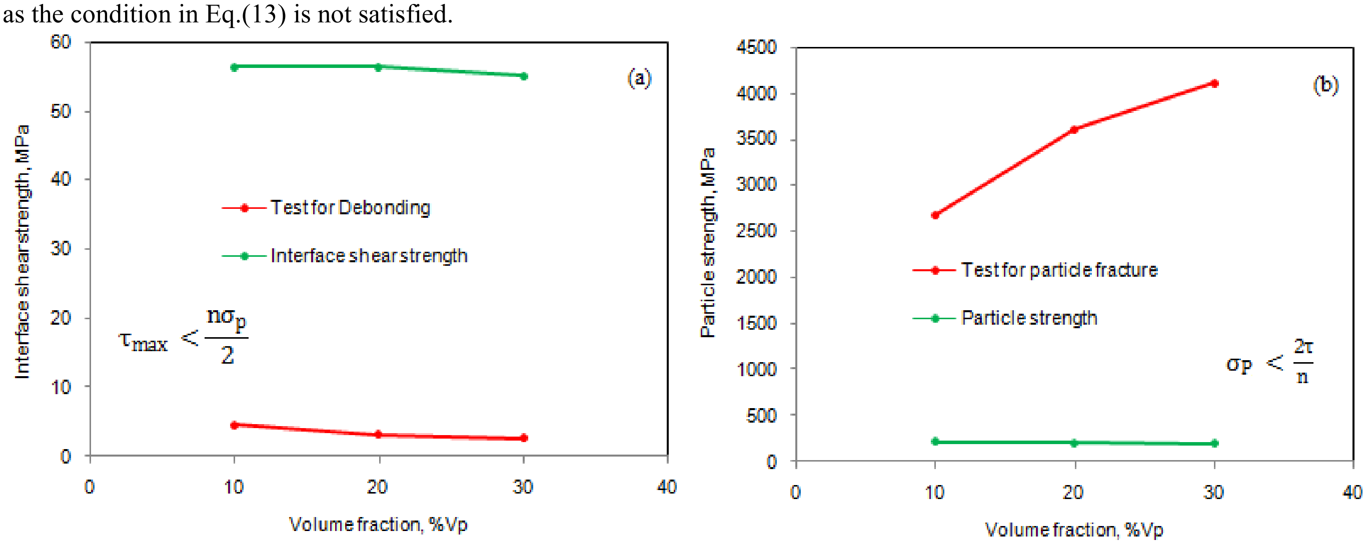

Figure 4: Criterion interfacial debonding (a) and for particle fracture (b).

As seen from 5 the von Mises stress developed in the matrix are lower than those induced in the nanoparticle. The von Mises stresses induced around the nanoparticle is much lower than those induced in the ZrC particle. Hence, the interfacial debonding was not occurred between the particle and the matrix. Owing to the high stress in the nanoparticles, the plastic deformation becomes concentrated at several locations in the matrix. The localized strain was observed around the particle because of the high load-transfer effect into the particles. Zirconium carbide (ZrC) is an extremely hard refractory ceramic material, commercially used in tool bits for cutting tools. The strong covalent Zr-C bond gives this material a very high melting point (~3530 °C), high modulus (430 GPa) and hardness (25 GPa).

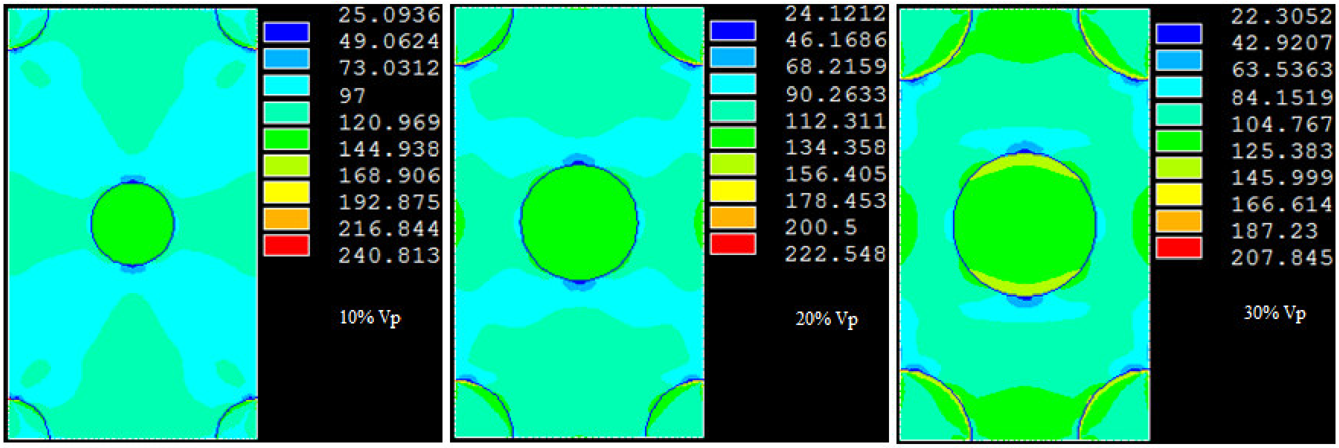

Figure 5: Images of von Mises Stress obtained from FEA.

5. CONCLUSION

There is likelihood of ZrC nanoparticle fracture in the AA1100/ZrC composites. The strong covalent Zr-C bond gives this material high modulus (430 GPa) and hardness (25 GPa). The difference between the FEA results and the test results can be attributed to the presence of voids in the composites and distribution of particles in the matrix.

REFERENCES

1. A. Chennakesava Reddy, Assessment of Debonding and Particulate Fracture Occurrences in Circular Silicon Nitride Particulate/AA5050 Alloy Metal Matrix Composites , National Conference on Materials and Manufacturing Processes, Hyderabad, India, 27-28 February 1998, pp. 104-109.
2. S. Sundara Rajan, A. Chennakesava Reddy, Deformation Behavior of AA8090/ TiO2 Nanoparticulate Reinforced Metal Matrix Composites with Debonding Interfaces, 2nd International Conference on Composite Materials and Characterization, Nagpur, India, 9-10 April 1999, pp. 245-248.
3. A. Chennakesava Reddy, Micromechanical Modelling of Interfacial Debonding in AA1100/Graphite Nanoparticulate Reinforced Metal Matrix Composites, 2nd International Conference on Composite Materials and Characterization, Nagpur, India, 9-10 April 1999, pp. 249-253.
4. A. Chennakesava Reddy, Local Stress Differential for Particulate Fracture in AA2024/Titanium Carbide Nanoparticulate Metal Matrix Composites, National Conference on Materials and Manufacturing Processes, Hyderabad, India, 27-28 February 1998, pp. 127-131.
5. H. B. Niranjan, A. Chennakesava Reddy, Effect of Particulate Debonding in AA5050/Boron Nitride Nanoparticulate Reinforced Metal Matrix Composites, 2nd International Conference on Composite Materials and Characterization, Nagpur, India, 9-10 April 1999, pp. 230-234.
6. P. M. Jebaraj, A. Chennakesava Reddy, Interface Debonding Prediction Technique for Tensile Loaded AA6061/Zirconium Oxide Nanoparticulate MMC, 2nd International Conference on Composite Materials and Characterization, Nagpur, India, 9-10 April 1999, pp. 235-239.
7. S. Sundara Rajan, A. Chennakesava Reddy, FEM Model for Volume Fraction Dependent Interface Debonding in TiN Nanoparticle Reinforced AA7020 Metal Matrix Composites, 2nd International Conference on Composite Materials and Characterization, Nagpur, India, 9-10 April 1999, pp. 240-244.
8. A. Chennakesava Reddy, Interfacial Debonding Analysis in Terms of Interfacial Tractions for Titanium Boride/AA3003 Alloy Metal Matrix Composites, 1st National Conference on Modern Materials and Manufacturing , Pune, India, 19-20 December 1997, pp. 124-127.
9. B. Kotiveera Chari, A. Chennakesava Reddy, Interfacial Debonding Analysis in Nanoparticulate Reinforced Metal Matrix Composites of AA8090/Zirconium Carbide, 2nd International Conference on Composite Materials and Characterization, Nagpur, India, 9-10 April 1999, pp. 210-214.

10. A. Chennakesava Reddy, Cohesive Zone Finite Element Analysis to Envisage Interface Debonding in AA7020/Titanium Oxide Nanoparticulate Metal Matrix Composites , 2nd International Conference on Composite Materials and Characterization, Nagpur, India, 9-10 April 1999, pp. 204-209.
11. A. Chennakesava Reddy, Evaluation of Debonding and Dislocation Occurrences in Rhombus Silicon Nitride Particulate/AA4015 Alloy Metal Matrix Composites, 1st National Conference on Modern Materials and Manufacturing , Pune, India, 19-20 December 1997, pp. 278-282.
12. H. B. Niranjan, A. Chennakesava Reddy, Debonding Failure and Volume Fraction Effects in Nano-reinforced Composites of AA2024/Silicon Oxide, 2nd International Conference on Composite Materials and Characterization, Nagpur, India, 9-10 April 1999, pp. 215-219.
13. B. Kotiveera Chari, A. Chennakesava Reddy, Effect of Debonding on Overall Behavior of AA3003/Titanium Carbide Nanoparticulate Reinforced Metal Matrix Composites, 2nd International Conference on Composite Materials and Characterization, Nagpur, India, 9-10 April 1999, pp. 220-224.
14. P. M. Jebaraj, A. Chennakesava Reddy, Analysis of Debonding along Interface of AA4015/Magnesium Oxide Nanoparticulate Reinforced Metal Matrix Composites, 2nd International Conference on Composite Materials and Characterization, Nagpur, India, 9-10 April 1999, pp. 225-229.
15. R. Hill, Elastic Properties of Reinforced Solids: Some Theoretical Principles, Engineering Journal of the Mechanics and Physics of Solids, Pergamon Press Ltd. Great Britain, 11, 1963, pp. 357-372.
16. Z. Hashin, Analysis of composite materials, A survey", Journal of Applied Mechanics, 50, 1983, pp. 481-505.
17. B. Kotiveerachari, A. Chennakesava Reddy, Interfacial effect on the fracture mechanism in GFRP composites, CEMILAC Conference, Ministry of Defence, India, 20-21st August 1999.